INSTITUTE OF PHYSICS PUBLISHING NANOTECHNOLOGY
Nanotechnology **17** (2006) 1668–1673 doi:10.1088/0957-4484/17/6/022

Large-scale production of carbon-coated copper nanoparticles for sensor applications

E K Athanassiou, R N Grass and W J Stark

Institute for Chemical and Bioengineering, ETH Zurich, 8093 Zurich, Switzerland

E-mail: wendelin.stark@chem.ethz.ch

Received 9 January 2006, in final form 30 January 2006
Published 27 February 2006
Online at stacks.iop.org/Nano/17/1668

Abstract
Copper nanoparticles with a mean carbon coating of about 1 nm were continuously produced at up to 10 g h^{-1} using a modified flame spray synthesis unit under highly reducing conditions. Raman spectroscopy and solid state ^{13}C magic angle spinning nuclear magnetic resonance spectroscopy revealed that the thin carbon layer consisted of a sp^2-hybridized carbon modification in the form of graphene stacks. The carbon layer protected the copper nanoparticles from oxidation in air. Bulk pills of pressed carbon/copper nanoparticles displayed a highly pressure- and temperature-dependent electrical conductivity with sensitivity at least comparable to commercial materials. These properties suggest the use of thin carbon/copper nanocomposites as novel, low-cost sensor materials and offer a metal-based alternative to the currently used brittle oxidic spinels or perovskites.

M Supplementary data files are available from stacks.iop.org/Nano/17/1668

(Some figures in this article are in colour only in the electronic version)

1. Introduction

Copper nanoparticles have attracted considerable interest because of their optical, catalytic, mechanical and electrical properties, resulting in a wide range of applications in the field of metallurgy, catalysis, nano- and optoelectronics [1–4]. Consequently, a wealth of preparation methods have been developed and range from wet phase preparations, hydrothermal, sonochemical or chemical reduction [1, 5–10] to gas phase processes [11–17]. In order to protect the sensitive metal nanoparticles from oxidation, they have been encapsulated in carbon/silica, polyethylene and pure carbon [12, 18–26].

In order to provide application-scale quantities of such carbon/copper nanomaterials, low-cost continuous preparation methods are required [18]. Since numerous oxide nanoparticles are manufactured industrially by flame synthesis in the kilogram to ton scale, we decided to investigate the use of a flame spray-based process for the synthesis of carbon-protected copper nanoparticles. In order to obtain metallic copper, previous studies on thermal decomposition of copper acetylacetonate have shown that a highly reducing atmosphere is required [12]. Since conventional flame spray synthesis is applied under ambient air, only oxides, salts or noble metals were obtainable [27–32]. As an indication, soot-forming flames provide a reducing environment, and they have been used for the preparation of carbon nanotubes in flames [33, 34]. We therefore investigated the construction of a continuously operating flame spray reactor within a nitrogen-filled glove-box to allow controlled flame synthesis even under highly reducing conditions. The setup was then used for the continuous large-scale production (10–100 g samples) of carbon-coated copper nanoparticles. In contrast to earlier studies that provided materials consisting predominantly of carbon, the use of reducing flame spray synthesis allowed the preparation of carbon layers on copper nanoparticles that are only 1 nm thick. In order to illustrate one possible novel application of this material we measured the bulk electrical properties of pressed C/Cu nanoparticles for a range of temperatures and pressures. The specific geometry of the C/Cu nanoparticles provided highly temperature- and pressure-

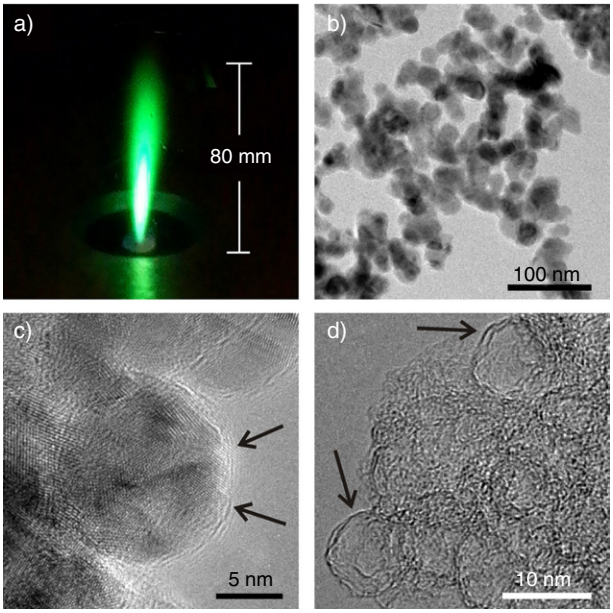

Figure 1. Flame spray synthesis of C/Cu nanoparticles under highly reducing conditions (a). Electron microscopy images of as-prepared ((b), (c)) particles. Treatment with nitric acid removed the copper core and resulted in carbon shells (d).

sensitive conductivity, which was at least comparable or superior to that of the currently used oxide-based spinels or perovskites.

2. Experiments

2.1. Reducing flame synthesis

A flame spray nozzle [35] consisting of a liquid spray surrounded by a premixed methane flame was placed in a glove-box (see supplementary information available at stacks.iop.org/Nano/17/1668) fed with nitrogen (N_2 atmosphere, O_2 < 100 ppm) and recirculated by a vacuum pump (Seco SV1040CV, Busch) at about 20 $m^3\,h^{-1}$. A mixture of Cu(II)-2-ethylhexanoate (5 wt% Cu in 2-ethyl hexanoic acid) and Tetrahydrofurane (2:1, by volume) was pumped at 4.5 $ml\,min^{-1}$ (HNP Mikrosysteme) into the spray nozzle of the flame reactor. The liquid was dispersed using an oxygen jet (5 $l\,min^{-1}$, Pangas tech). The resulting spray was ignited by a methane–oxygen pilot flame (CH_4 1.2 $l\,min^{-1}$, O_2 2.2 $l\,min^{-1}$, Pangas tech). The green-coloured flame (figure 1(a)) converted the liquid copper carboxylate solution into carbon/copper nanoparticles that were collected above the flame on a water-cooled glass fibre filter. The combustion products CO_2 and H_2O were removed continuously from the gas stream using two adsorption columns packed with 50 kg zeolite 4A and 13X (Zeochem), respectively. To avoid the accumulation of CO, NO and other impurities in the glove-box atmosphere a purge gas stream (1–4 $m^3\,h^{-1}$) continuously passed the box. A mass spectrometer (Balzers GAM 400) was applied for detection of the concentrations of H_2, N_2, CO_2, NO, NO_2 and O_2 gas.

Since no additional oxygen is provided from the nitrogen atmosphere in the glove-box the overall content of oxygen entering the flame is predefined by the operating conditions (see above). The degree of oxidation in the flame process may therefore be characterized by the fuel to oxygen ratio Φ which is defined as

$$\Phi = \frac{\text{moles of oxygen required for complete combustion}}{\text{moles of oxygen available}}.$$

2.2. Physical and electrical properties

The C/Cu and carbon shells were analysed by a series of physical methods: x-ray diffraction (XRD) (Siemens powder x-ray diffractometer with a Ni-filtered Cu Kα radiation, step size 0.3°), nitrogen adsorption (BET) (Tristar Micromeritics Instruments), transmission electron microscopy (TEM) (CM30 ST-Philips, LaB_6 cathode, operated at 300 kV point resolution ~2 Å), solid state ^{13}C magic angle spinning (MAS) nuclear magnetic resonance (NMR) (Bruker Ultra Shield NMR spectrometer, operated at 500 MHz) and Raman spectroscopy (Bruker EQUINOX 55, 790 nm laser source). Conductivity measurements were conducted according to [36] using four measuring points on correspondingly pressed tablets of the powder.

For the preparation of carbon shells, samples of the as-produced C/Cu powder were dissolved in a 50 wt% nitric acid solution and stirred for 30 min, filtered and washed repeatedly with ultrapure water (Millipore). After drying under air at 100 °C, the carbon shells were heated to 400 °C for 30 min under vacuum to remove any remaining traces of water.

3. Results

3.1. Synthesis of C/Cu nanoparticles

The operation of a flame spray setup under a nitrogen atmosphere at a fuel to oxygen ratio of 1.5 resulted in the conversion of methane/oxygen and the spray liquid (2-ethylhexanoic acid and tetrahydrofurane) into a gas mixture containing several volume per cent of carbon monoxide and hydrogen next to water and carbon dioxide (figure 1(a)). This reducing flame synthesis is in clear contrast to conventional flame spray synthesis which exclusively produces water and carbon dioxide. No remaining oxygen could be detected by mass spectroscopy in the off-gas from the flame (detection limit <10 ppm) and confirmed a thorough conversion of oxygen in the flame reactor. Introduction of a soluble copper precursor into the liquid fuel resulted in the formation of a fine black powder that could be collected on the top of the flame using temperature-resistant glass-fibre filters.

3.2. Physical properties of C/Cu

Transmission electron microscopy of the C/Cu powder showed that the product consisted of nanoparticles with a diameter of 10–20 nm (figure 1(b)). The surface of the copper was covered by a thin carbon layer (figure 1(c)) as further evidenced by element-sensitive mapping (supplementary information available at stacks.iop.org/Nano/17/1668) and energy dispersive x-ray spectroscopy (EDX). The powder exhibited a specific surface area as measured by the BET method of 67 $m^2\,g^{-1}$. The product showed no apparent reactivity towards oxygen if exposed to air at

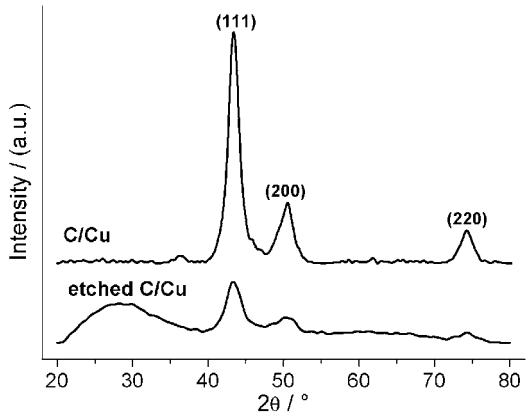

Figure 2. X-ray diffraction pattern of as-prepared C/Cu nanoparticles (first trace) displaying pronounced peaks assigned to metallic copper. Partially HNO_3 etched C/Cu (second trace) shows much weaker signals for copper and an amorphous contribution at 20°–40°.

room temperature, as confirmed by thermogravimetry. X-ray diffraction (figure 2, C/Cu) corroborated the presence of metallic copper. In order to better characterize the carbon layer, the copper core was removed by washing the C/Cu composite using highly oxidizing and protonating conditions (50 wt% HNO_3). X-ray diffraction (figure 2, etched) and chemical analysis by titration confirmed that the treatment removed most of the copper core.

Transmission electron microscopy showed that the etching had resulted in hollow carbon nanoshells (figure 1(d)). The XRD pattern of as-prepared material (figure 2) showed no evidence of copper oxides or carbides in any sample.

3.3. Physical properties of carbon shells

The XRD pattern of the carbon shells displayed a broad peak around 20°–40° indicating the presence of a non-crystalline material. No peak for graphite could be detected. Similar XRD patterns (20°–40°) have been observed for amorphous carbon, multiwall carbon nanotubes [37] and glassy carbon modifications [38].

The carbon nanoshells were therefore further investigated by nuclear magnetic resonance and Raman spectroscopy (figure 3). Magic angle spinning ^{13}C-NMR spectra showed wide signals around 100–140 ppm for the as-prepared product and between 70 and 140 ppm for the etched sample (figure 3(a)). These regions correspond to sp^2-hybridized carbon. The presence of graphite [39] would give rise to a signal around $\delta = 180$ ppm and could therefore be excluded. Single-wall carbon nanotubes (SWNT, [39], δ 121–126 ppm) and multiwall carbon nanotubes (MWNT, [40], δ 121–130 ppm) give rise to NMR spectra in a similar region. This indicates that the carbon is similar to carbon nanotubes.

Since all carbon modifications show distinct Raman signals, the carbon shells were further measured for their Raman spectra (figure 3(b)). The as-prepared C/Cu (figure 3(b), trace 1) and the carbon shells after etching (figure 3(b), trace 2) displayed broad absorption bands at around 1600 and 1300 cm^{-1}. The Raman spectra of commercial SWNT (Elicarb, figure 3(b), trace 3) as a reference may be characterized by the appearance of the so-called D-line at 1284 cm^{-1} and G-line at 1594 cm^{-1} [41]. Nemanich

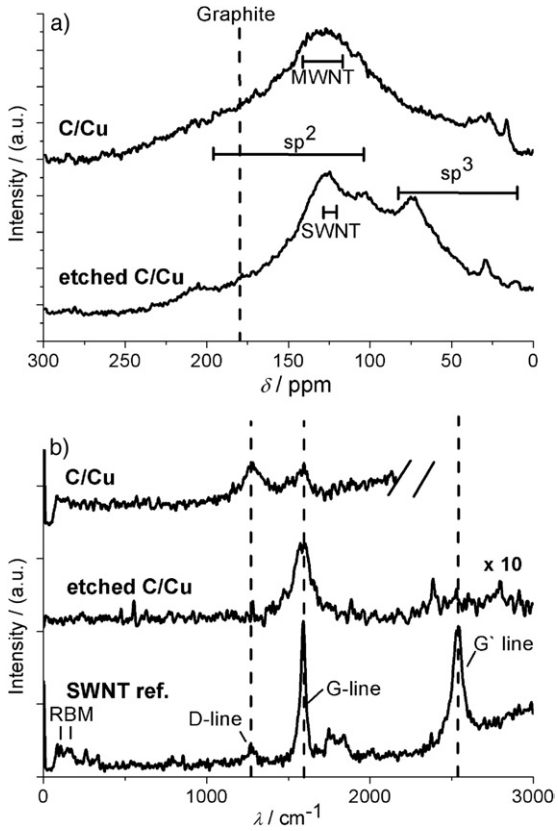

Figure 3. (a) ^{13}C-MAS-NMR spectra and (b) Raman spectra of the as-prepared product (first trace), etched carbon shells (second trace) and commercial SWNT (third trace). The G-line characteristic for ordered graphene layers was found in all samples.

and Solin [42] assigned the G-line to the E_{2g} mode involving two adjacent C atoms in a graphene sheet. The G-line has been used as a characteristic band for ordered graphite carbon sheets. The D-line has been accredited to a size effect with growing intensity for smaller crystallite size [43] and was observed in nanotube-like carbon modifications and glassy carbon [44]. The Raman spectrum of the as-prepared C/Cu powder (figure 3(b), 1st trace) shows both lines at a similar intensity. Upon etching of carbon-coated copper nanoparticles, the intensity of the D-line strongly decreased (second trace) indicating a more ordered carbon arrangement and the formation of an ordered graphite-like structure [38]. A clear difference from SWNT arises from the lack of the characteristic radial breathing mode (RBM) lines (A_{1g} 'breathing' mode) [45].

The mean thickness of the carbon layer can be calculated from the carbon content of the material (17.5%) and its specific surface area (67 $m^2\ g^{-1}$) assuming a density of carbon of about 2200 kg m^{-3}. The mean carbon layer thickness is therefore calculated as $d_{carbon} = 0.175/\rho/A_{BET}$, resulting in an average layer thickness of 1.2 nm.

3.4. Pressure- and temperature-dependent conductivity

Pressing the as-prepared powder uniaxially at 370 MPa into a pill (figure 4(a)) resulted in a dark solid material with some metallic gloss. For reference we included pressed, commercial micrometre-sized copper (350–450 μm,

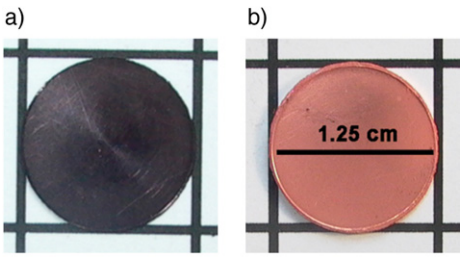

Figure 4. About 1 nm carbon-coated copper pressed at 370 MPa (a) and micrometre-sized pure copper (b).

figure 4(b)). Conductivity measurements on the bulk C/Cu were done for increasing pressure at 295 K and at constant pressure for temperatures from 60 to 373 K. The specific resistance rapidly and reversibly (figure S3) dropped upon increasing pressures and showed a strong power law correlation (figure 5(a), $\rho(\mathrm{k\Omega\ m}) = 3.2 \times P\ (\mathrm{bar})^{-0.76}$) over four orders of magnitude similar to the conductivity most recently observed by Radhakrishnan [46] for an elastomer/polyaniline blend. Variations of the temperature strongly affected the conductivity of the C/Cu nanocomposite. The specific resistance decreased with increasing temperature (figure 5(b)), as measured using a four-point technique in an oxygen-free atmosphere (T_1: 55–304 K at high pressure and T_2: 304–373 K at low pressure). The C/Cu showed a strong negative temperature coefficient (NTC) behaviour, as found in commercial piezoelectric materials.

4. Discussion

Conventional flame synthesis is an industrially used process for manufacturing ton quantities of oxide nanoparticles and has been extended for the preparation of carbon-coated air-stable metallic copper nanoparticles. The preparation showed that flame spray synthesis could even be applied with a strongly limited oxygen supply in the combustion zone. The resulting off-gas composition was characterized by a lack of remaining oxygen, down to the ppm level, and a high content of reducing gases, such as hydrogen and carbon monoxide. Instead of forming copper oxide as in conventional flame spray synthesis, the highly reducing conditions resulted in the formation of zero-valent copper particles. These results agree with those of studies on the formation of carbon nanotubes in flames catalysed by metallic nickel or iron [33, 34, 47]. The reduction potential in such highly reducing flames is obviously sufficient to allow the presence of metallic nickel, iron or copper. The preparation of copper from copper 2-acetylacetonate by Nasibulin [12] further supports the feasibility of producing metallic copper under similar gas compositions as used in the present study. The high air stability of the C/Cu agrees well with the passivation of iron nanoparticles by carbon layers [48].

Following the detailed study by Nasibulin *et al* [12] of the decomposition of copper acetylacetonate under a series of CO-, water- or H_2-containing atmospheres, copper catalyses the deposition of carbon out of an atmosphere containing carbon monoxide. A similar reaction may be suggested to result in the deposition of carbon on the copper nanoparticles described here.

Etching of the copper core resulted in carbon shells (figure 1(d)) of unknown structure, motivating further analysis. X-ray diffraction revealed amorphous contributions indicating the possible formation of non-crystalline or glassy carbon (figure 2). This stands in contrast to the Raman spectra showing a strong G-band indicating ordered graphene structures. The absence of a D-band showed a clear difference from the disordered structures previously found in glassy, amorphous or carbon nanotube modifications [49]. It may therefore be concluded that the present carbon shells consisted of stacked, slightly ordered graphene layers. The thickness of the stack, about 1.2 nm, was too small to give a defined peak in the x-ray diffractogram. This is further supported by the NMR spectrum showing a wide range of sp^2-hybridized carbon species. The lack of evidence of the formation of bulk graphite from the NMR spectrum is in agreement with a previous study on the formation of giant fullerenes [50]. In contrast to the thick carbon multishells obtained by Schaper *et al* [21], the very thin layers of the present material may be used for the development of sensor materials. In comparison with earlier studies [12, 18, 21] the use of reducing flame spray synthesis allowed production of 10–100 g samples and therefore offers a cost-effective and scalable way to synthesize these most versatile nanomaterials.

The pronounced negative temperature conductivity (NTC) behaviour of bulk C/Cu revealed a characteristic material

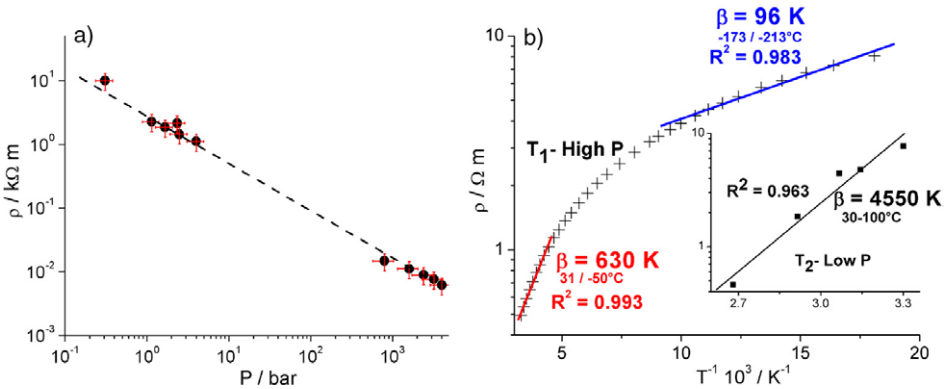

Figure 5. (a) Pressure dependence of the electrical resistivity. The resistivity follows a power law estimated as $\rho(\mathrm{k\Omega\ m}) = 3.2 \times P\ (\mathrm{bar})^{-0.76}$. (b) The temperature dependence of the resistivity shows a strong NTC behaviour. The corresponding material constant β was calculated for two experimental conditions (T_1, high pressure, and T_2, ambient pressure (inset)).

constant β of above 4500 K. The C/Cu nanomaterial therefore showed a similar or greater sensitivity than today's commercially applied ceramic sensing materials (Mn–Zn–Ni spinel: $\beta = 4261$ K, [51]; Ni–Co–Mn spinel: $\beta = 4451$ K [52]). The polyaniline/elastomer composite described by Radhakrishnan [46] represents a good conductor (polyaniline) dispersed in a poor electrical conductor (elastomer). The structure of pressed, about 1 nm carbon-coated metallic copper nanoparticles offers a similar geometry. We therefore observed a similar power law for the temperature-dependent conductivity (see figure 5). Extremely small gaps between copper nanoparticles arose from just a few layers of carbon (estimated thickness of about 2–3 nm). The NTC coefficient is therefore exceptionally large and gives rise to the high observed sensitivity. However, further investigations are required to elucidate the detailed mechanism of this effect.

5. Conclusion

The use of reducing flame spray synthesis proved very effective for the large-scale, one-step preparation of carbon-coated copper nanoparticles. The copper nanoparticles were stable in air due to the protection of about 1 nm carbon. The carbon layer consisted of sp^2-hybridized graphite stacks with a low degree of crystalline order and a spherical shape. The material may be pressed to bulk pills which exhibit highly pressure- and temperature-dependent conductivity. Since the observed sensitivity is at least comparable to currently used oxide materials, the C/Cu nanoparticles may offer an alternative sensor material for temperature and pressure sensing.

Acknowledgments

We thank C Mensing for the conductivity measurements and Dr H Rüegger for the NMR measurements. Financial support by the ETH Zürich is gratefully acknowledged.

References

[1] Dhas N A, Raj C P and Gedanken A 1998 Synthesis, characterization, and properties of metallic copper nanoparticles *Chem. Mater.* **10** 1446–52
[2] Vitulli G, Bernini M, Bertozzi S, Pitzalis E, Salvadori P, Coluccia S and Martra G 2002 Nanoscale copper particles derived from solvated Cu atoms in the activation of molecular oxygen *Chem. Mater.* **14** 1183–6
[3] Zhou D W 2004 Heat transfer enhancement of copper nanofluid with acoustic cavitation *Int. J. Heat Mass Transfer.* **47** 3109–17
[4] Quaranta A, Ceccato R, Menato C, Pederiva L, Capra N and Dal Maschio R 2004 Formation of copper nanocrystals in alkali-lime silica glass by means of different reducing agents *J. Non-Cryst. Solids* **345/46** 671–5
[5] Zhang D W, Yi T H and Chen C H 2005 Cu nanoparticles derived from CuO electrodes in lithium cells *Nanotechnology* **16** 2338–41
[6] Pileni M P and Lisiecki I 1993 Nanometer metallic copper particle synthesis in reverse micelles *Colloids Surf.* A **80** 63–8
[7] Lisiecki I, Sack-Kongehl H, Weiss K, Urban J and Pileni M P 2000 Annealing process of anisotropic copper nanocrystals. 1. Cylinders *Langmuir* **16** 8802–6
[8] Pileni M P, Ninham B W, Gulik-Krzywicki T, Tanori J, Lisiecki I and Filankembo A 1999 Direct relationship between shape and size of template and synthesis of copper metal particles *Adv. Mater.* **11** 1358–62
[9] Qi L M, Ma J M and Shen J L 1997 Synthesis of copper nanoparticles in nonionic water-in-oil microemulsions *J. Colloid Interface Sci.* **186** 498–500
[10] Kumar R V, Mastai Y, Diamant Y and Gedanken A 2001 Sonochemical synthesis of amorphous Cu and nanocrystalline Cu_2O embedded in a polyaniline matrix *J. Mater. Chem.* **11** 1209–13
[11] Huang H H, Yan F Q, Kek Y M, Chew C H, Xu G Q, Ji W, Oh P S and Tang S H 1997 Synthesis, characterization, and nonlinear optical properties of copper nanoparticles *Langmuir* **13** 172–5
[12] Nasibulin A G, Shurygina L I and Kauppinen E I 2005 Synthesis of nanoparticles using vapor-phase decomposition of copper(II) acetylacetonate *Colloid J.* **67** 1–20
[13] Ponce A A and Klabunde K J 2005 Chemical and catalytic activity of copper nanoparticles prepared via metal vapor synthesis *J. Mol. Catal.* A **225** 1–6
[14] Liu Z W and Bando Y 2003 A novel method for preparing copper nanorods and nanowires *Adv. Mater.* **15** 303–5
[15] Ullmann M, Friedlander S K and Schmidt-Ott A 2002 Nanoparticle formation by laser ablation *J. Nanopart. Res.* **4** 499–509
[16] Narayan R J 2005 Pulsed laser deposition of functionally gradient diamondlike carbon-metal nanocomposites *Diamond Relat. Mater.* **14** 1319–30
[17] Kazakevich P V, Voronov V V, Simakin A V and Shafeev G A 2004 Production of copper and brass nanoparticles upon laser ablation in liquids *Quantum Electron.* **34** 951–6
[18] Li C M, Lei H, Tang Y J, Luo J S, Liu W and Chen Z M 2004 Production of copper nanoparticles by the flow-levitation method *Nanotechnology* **15** 1866–9
[19] Xia X P, Cai S Z and Xie C S 2006 Preparation, structure and thermal stability of Cu/LDPE nanocomposites *Mater. Chem. Phys.* **95** 122–9
[20] Sergiienko R, Shibata E, Suwa H, Nakamura T, Akase Z, Murakami Y and Shindo D 2006 Synthesis of amorphous carbon nanoparticles and carbon encapsulated metal nanoparticles in liquid benzene by an electric plasma discharge in ultrasonic cavitation field *Ultrason. Sonochem.* **13** 6–12
[21] Schaper A K, Hou H, Greiner A, Schneider R and Phillipp F 2004 Copper nanoparticles encapsulated in multi-shell carbon cages *Appl. Phys.* A **78** 73–7
[22] Fu R W, Yoshizawa N, Dresselhaus M S, Dresselhaus G, Satcher J H and Baumann T F 2002 XPS study of copper-doped carbon aerogels *Langmuir* **18** 10100–4
[23] Qin Y, Zhang Q and Cui Z L 2004 Effect of synthesis method of nanocopper catalysts on the morphologies of carbon nanofibers prepared by catalytic decomposition of acetylene *J. Catal.* **223** 389–94
[24] Xu C L, Wu G W, Liu Z, Wu D H, Meek T T and Han Q Y 2004 Preparation of copper nanoparticles on carbon nanotubes by electroless plating method *Mater. Res. Bull.* **39** 1499–505
[25] Subramoney S 1998 Novel nanocarbons—structure, properties, and potential applications *Adv. Mater.* **10** 1157
[26] Saito Y 1995 Nanoparticles and filled nanocapsules *Carbon* **33** 979–88
[27] Rosner D E 2005 Flame synthesis of valuable nanoparticles: Recent progress/current needs in areas of rate laws, population dynamics, and characterization *Ind. Eng. Chem. Res.* **44** 6045–55
[28] Stark W J and Pratsinis S E 2002 Aerosol flame reactors for manufacture of nanoparticles *Powder Technol.* **126** 103–8
[29] Makela J M, Keskinen H, Forsblom T and Keskinen J 2004 Generation of metal and metal oxide nanoparticles by liquid flame spray process *J. Mater. Sci.* **39** 2783–8

[30] Grass R N and Stark W J 2005 Flame synthesis of calcium-, strontium-, barium fluoride nanoparticles and sodium chloride *Chem. Commun.* 1767–9
[31] Laine R M, Marchal J, Sun H P and Pan X Q 2005 A new Y3Al5O12 phase produced by liquid-feed flame spray pyrolysis (LF-FSP) *Adv. Mater.* **17** 830
[32] Loher S, Stark W J, Maciejewski M, Baiker A, Pratsinis S E, Reichardt D, Maspero F, Krumeich F and Gunther D 2005 Fluoro-apatite and calcium phosphate nanoparticles by flame synthesis *Chem. Mater.* **17** 36–42
[33] Vander Wal R L 2002 Fe-catalyzed single-walled carbon nanotube synthesis within a flame environment *Combust. Flame* **130** 37–47
[34] Height M J, Howard J B, Tester J W and Sande J B V 2004 Flame synthesis of single-walled carbon nanotubes *Carbon* **42** 2295–307
[35] Madler L, Kammler H K, Mueller R and Pratsinis S E 2002 Controlled synthesis of nanostructured particles by flame spray pyrolysis *J. Aerosol. Sci.* **33** 369–89
[36] Hu C Y, Gao Y Q and Sheng Z Y 2000 The piezoresistance coefficients of copper and copper–nickel alloys *J. Mater. Sci.* **35** 381–6
[37] Guo D J and Li H L 2005 Highly dispersed Ag nanoparticles on functional MWNT surfaces for methanol oxidation in alkaline solution *Carbon* **43** 1259–64
[38] Wang X, Zhang G M, Zhang Y L, Li F Y, Yu R C, Jin C Q and Zou G T 2003 Graphitization of glassy carbon prepared under high temperatures and high pressures *Carbon* **41** 188–91
[39] Goze-Bac C, Latil S, Lauginie P, Jourdain V, Conard J, Duclaux L, Rubio A and Bernier P 2002 Magnetic interactions in carbon nanostructures *Carbon* **40** 1825–42
[40] Kishinevsky S, Nikitenko S I, Pickup D M, van-Eck E R H and Gedanken A 2002 Catalytic transformation of carbon black to carbon nanotubes *Chem. Mater.* **14** 4498–501
[41] Mamedov A A, Kotov N A, Prato M, Guldi D M, Wicksted J P and Hirsch A 2002 Molecular design of strong single-wall carbon nanotube/polyelectrolyte multilayer composites *Nat. Mater.* **1** 190–4
[42] Nemanich R J and Solin S A 1979 1st-order and 2nd-order raman-scattering from finite-size crystals of graphite *Phys. Rev.* B **20** 392–401
[43] Tuinstra F and Koenig J L 1970 Raman spectrum of graphite *J. Chem. Phys.* **53** 1126
[44] Hiura H, Ebbesen T W, Tanigaki K and Takahashi H 1993 Raman studies of carbon nanotubes *Chem. Phys. Lett.* **202** 509–12
[45] Qian W Z, Liu T, Wei F and Yuan H Y 2003 Quantitative Raman characterization of the mixed samples of the single and multi-wall carbon nanotubes *Carbon* **41** 1851–4
[46] Radhakrishnan S and Kar S B 2005 Role of non-linear processes in conducting polymer blends for piezo-sensors Part 2: Studies on polyaniline/SBS blends *Sensors Actuators* A **120** 474–81
[47] Vander Wal R L 2002 Flame synthesis of Ni-catalyzed nanofibers *Carbon* **40** 2101–7
[48] Vander Wal R L 2000 Flame synthesis of substrate-supported metal-catalyzed carbon nanotubes *Chem. Phys. Lett.* **324** 217–23
[49] Eklund P C, Holden J M and Jishi R A 1995 Vibrational-modes of carbon nanotubes—spectroscopy and theory *Carbon* **33** 959–72
[50] Selvan R, Unnikrishnan R, Ganapathy S and Pradeep T 2000 Macroscopic synthesis and characterization of giant fullerenes *Chem. Phys. Lett.* **316** 205–10
[51] Yue Z X, Qi X W, Wang X H, Zhou J, Gui Z L and Li L T 2002 Low-temperature sintered Ni–Zn manganite NTC ceramics prepared by a gel auto-combustion method *J. Mater. Sci. Lett.* **21** 375–7
[52] Park K and Bang D Y 2003 Electrical properties of Ni–Mn–Co–(Fe) oxide thick-film NTC thermistors prepared by screen printing *J. Mater. Sci., Mater. Electron.* **14** 81–7